One year of continuous dynamic monitoring of a football stadium suspension roof: analysis of data provided by an autonomous monitoring application

S. Amador, N. Martins, F. Magalhães, E. Caetano, A. Cunha
ViBest, Faculty of Engineering, University of Porto,
Rua Dr. Roberto Frias, s/n 4200-465 Porto, Portugal
e-mail: **sandro.diord@fe.up.pt**

Abstract

In recent years, significant effort has been made to improve the assessment of the health condition of civil engineering structures by means of vibration measurements acquired in permanent monitoring. One of the main obstacles to achieve this goal is the development and implementation of an autonomous application which is capable of extracting relevant information out of the large amount of data collected continuously, regardless of the influence of the environmental effects (e. g. temperatures, wind, etc.). In this context, the present paper describes the most relevant results obtained along one year of permanent dynamic monitoring of a suspension roof. The monitored structure corresponds to the roof of a football stadium which is basically composed by two concrete slabs suspended by 34 pairs of full locked coil cables. The stadium is located in the city of Braga, Portugal, and its suspension roof has been permanently monitored by the Laboratory of Vibrations and Structural Monitoring (**ViBest**) of the Faculty of Engineering of University of Porto (FEUP) since March 2009. After the installation of the monitoring system on the west slab, the dynamic properties of the structure have been automatically tracked with very few failures. Therefore, apart from describing the results obtained along one year of monitoring, this paper also outlines the major aspects concerning the tools which were especially created to automatically acquire and process the data, remove the environmental effects, and extract useful information to assess the health condition of the monitored structure.

1 Introduction

One of the main challenges to assess the health and integrity of civil engineering structures by means of the dynamic responses is the transformation of the data continuously collected by the monitoring systems into relevant information regarding the structural condition of the monitored structures. The most important step to achieve this goal is the implementation of a robust and accurate automated monitoring application to process the raw data files and extract such information from the large amount of data available in such monitoring. Considerable efforts have been made towards this objective in an attempt to develop a robust, accurate and reliable fully automated monitoring system as seen, for instance, in [1, 2, 3]. In this context, this paper describes some features of the autonomous monitoring system which was implemented to assess the health condition of a suspension roof of a football stadium located in the city of Braga, Portugal. The suspension roof consists of two concrete slabs supported by 34 pairs of full locked coil cables with diameters ranging from 80 to $86\,mm$ as illustrated in Figure 1. Several studies were carried out by the Laboratory of Vibrations and Monitoring (**ViBest**, http://www.fe.up.pt/vibest) of the Faculty of Engineering of the University of Porto (FEUP) to assess the structural behavior of the suspension roof under varying environmental conditions since the beginning of the structural design [4, 5, 6]. The results provided by such studies as well as those obtained from the numerical simulations and wind tunnel tests performed during the early stage of

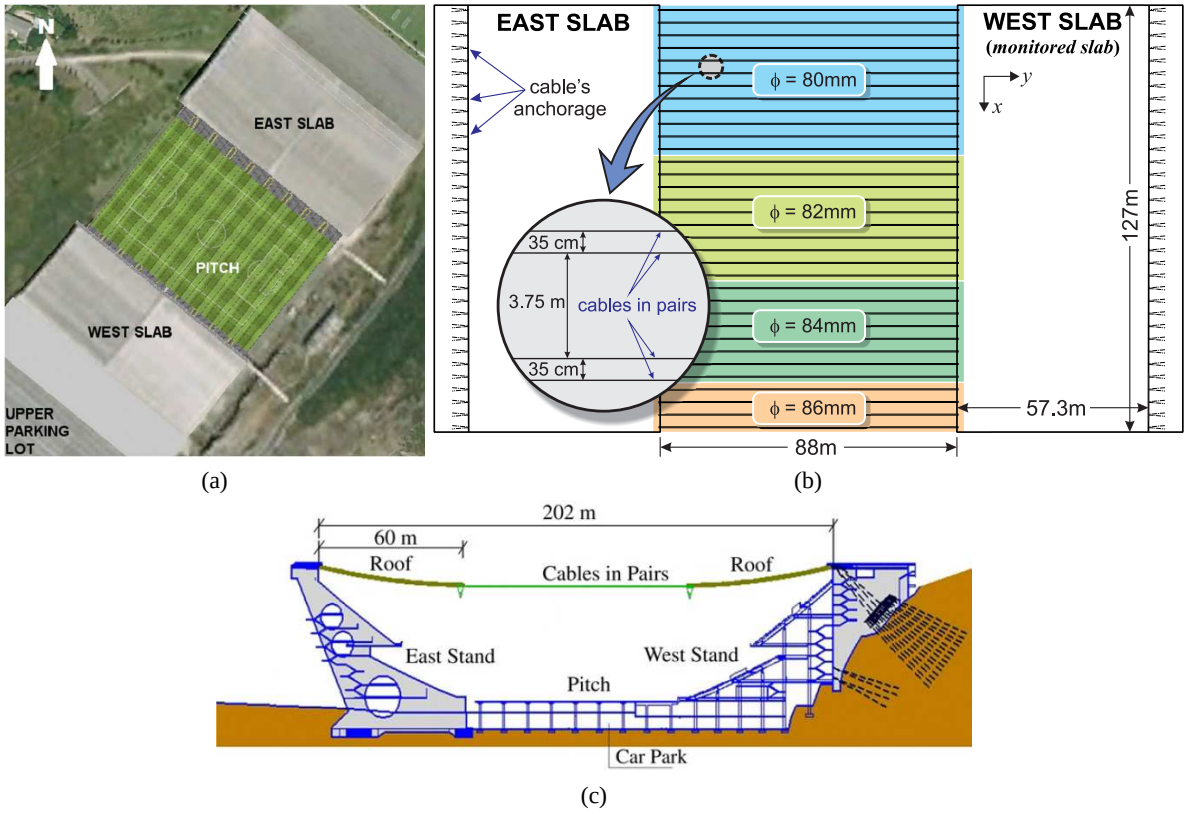

Figure 1: Braga football stadium: (a) position of the stadium (top view); (b) distribution of the suspension cables (top view); and (c) schematic lateral view.

the structural design have demonstrated that the structure could be vulnerable to aeroelastic instabilities [7]. These conclusions have motivated the installation of a continuous dynamic monitoring system to assess the effects of the environmental actions on the structural performance of the suspension roof along the time. This system comprises a set of force balance accelerometers, a robust data acquisition system and an autonomous monitoring application which was created to extract relevant information concerning the integrity of the monitored structure. In operation since March, 2009, this system has already provided interesting results concerning the effects of the environmental actions on the dynamic properties of the suspension roof [8] and the results acquired along one year of permanent dynamic monitoring are shown in this paper to demonstrate the efficiency of the implemented system. More recently, at the beginning of December, 2011, another monitoring system was installed on the suspension roof to assess the influence of the wind loading on the dynamic behavior of the roof structure [9]. The analysis of the data provided by this wind monitoring system, in combination with the data from dynamic monitoring system, provided useful results regarding the effects of wind on the dynamic properties of the suspension roof.

2 Operational modal analysis

An ambient vibration test of the roof structure with a high spatial resolution was carried out in May, 2011, to identify the modal properties of the roof structure in its undamaged condition, creating a baseline reference subsequently used by the autonomous monitoring application described in 3.3. The test took place only on the west slab using a set of six tri-axial seismographs and six uni-axial accelerometers, and was conducted using 15 different setups, which involved 6 moving seismographs and the 6 fixed reference accelerometers that integrate the permanent dynamic monitoring system described in section 3.2. The sensors were placed in order to measure the vertical accelerations of a total of 90 points on the slab.

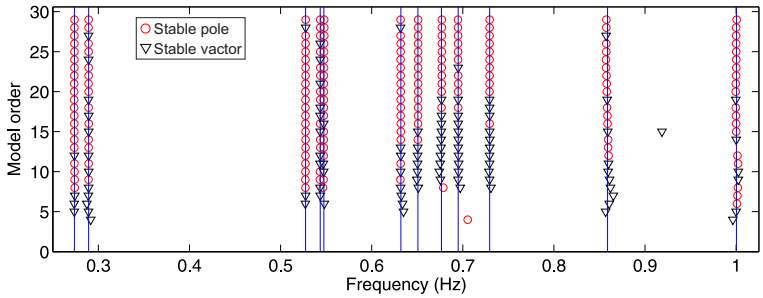

Figure 2: Stability diagram of the merged data constructed with the p-LSCF technique

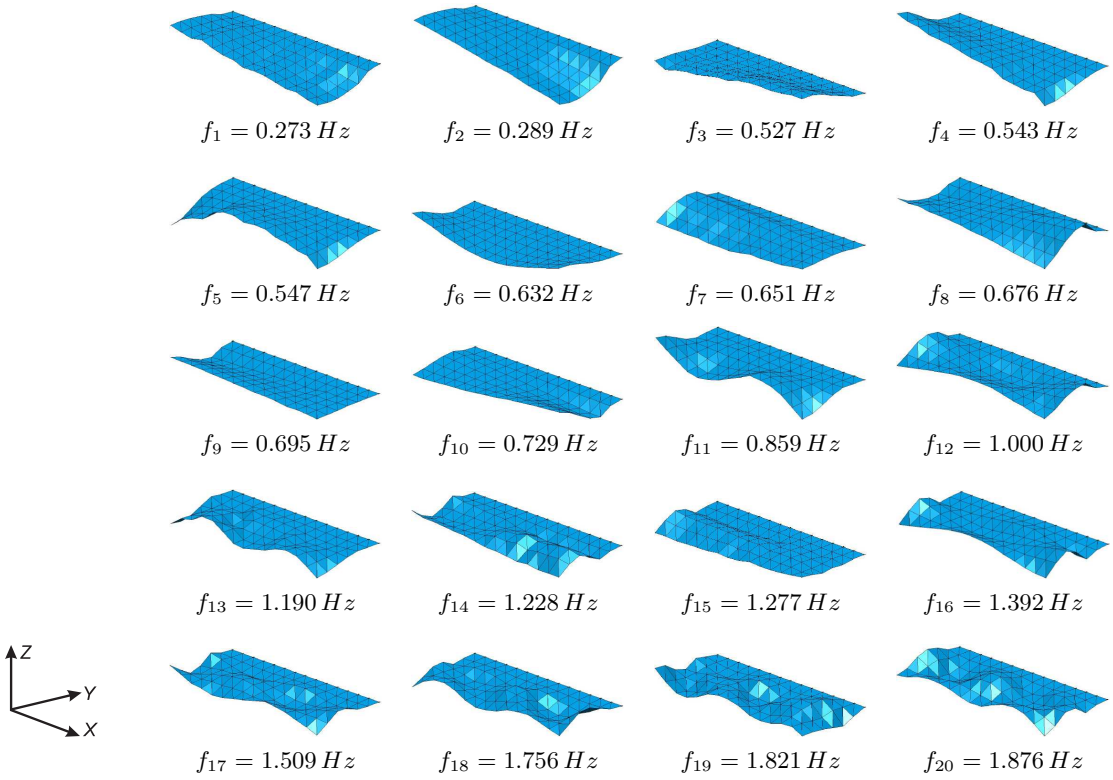

Figure 3: Natural frequencies and the corresponding mode shapes of the west slab experimentally identified by using the p-LSCF technique.

Further details about this test can be found in [8]. Each setup time series was acquired with sampling frequencies of 100 and 20 Hz for the rover sensors and the reference sensors, respectively. The difference between these sampling frequencies is explained by the fact that two different acquisition systems were used. Still, a good synchronization between both systems was possible thanks to the use of GPS embedded in both systems. The modal parameters were then determined in the frequency range of $0 - 2\,Hz$ using **O**perational **M**odal **A**nalysis **Studio** (**OMA studio**) Toolbox [10], according to the following steps: (i) synchronization of each setup time series collected by the moving sensors with regard to their reference counterparts, as these signals were acquired by different acquisition systems; (ii) pre-processing and estimation of the half spectra matrices for each setup using the so-called *weighted correlogram* with 512 time lags to calculate the correlation matrices [11]; (iii) merging of these spectra matrices in one single matrix using **P**ost **G**lobal **E**stimation (**PoGER**) technique [12, 13]; (iv) Identification of the natural frequencies, damping ratios and the corresponding operational factors of all the merged setups at once by means of **P**oly Reference **L**east **S**quares **C**omplex **F**requency **D**omain (**p-LSCF**) identification method [11]; (v) re-scaling of the operational factors of each setup with regard to the first setup; and, finally, (vi) estimation of the mode shapes using the well-known **L**east **S**quares **F**requency **D**omain (**LSFD**) estimator [11]. A stability diagram in the frequency range

of $0-1\,Hz$ obtained by following the aforementioned procedure is shown in Figure 2. The remaining modal parameters corresponding to the frequency range of $1-2\,Hz$ were identified using another stability diagram that was constructed in the frequency band of $0-2\,Hz$. The natural frequencies and the corresponding mode shapes experimentally identified in the frequency range of $0-2\,Hz$ are shown in Figure 3. These parameters were automatically obtained by means of a hierarchical clustering algorithm [14] described in section 3.3.

3 Continuous monitoring of the roof structure

The roof structure is currently monitored by two different systems (Figure 4): one to monitor the dynamic response and the other to collect wind measurements. In operation since March, 2009, the continuous dynamic monitoring system is set to acquire the vertical acceleration by means of 6 force-balance accelerometers. The wind monitoring system was installed in the beginning of December, 2011, and is composed by two ultrasonic anemometers that are suitable to measure the ambient temperatures, velocity and direction of the wind at high sampling frequencies. This new independent and complementary wind measurement system was installed on the west slab of the stadium in order to characterize the wind model and analyze correlations between the structure's dynamic response and the wind load.

The installation of both monitoring systems comprised several elements as described in Figure 4. The correlation between the data provided by both systems has allowed the assessment of the complex non-linear interactions between the monitored structure and the environmental effects.

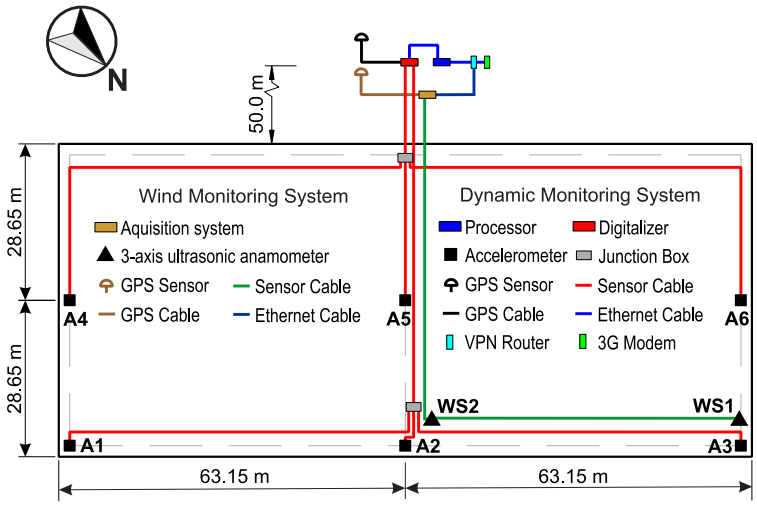

Figure 4: Location of components of the two monitoring systems installed for wind measurements and acquisition of vertical accelerations on the Braga stadium suspension roof (top view of the west slab).

3.1 Wind measurement system

This system comprehends two three-dimensional ultrasonic anemometers which allow the characterization of the wind through time averaged statistics of speed, direction and incidence angles, spectra and co-spectra of velocity components and temperature. These quantities can be subsequently used to assess the influence of the wind loading on the dynamic behavior of the roof structure. According to the scheme and picture presented in Figure 4, the two anemometers were placed on the top of the west slab, both along its inner edge, **WS1** in the northernmost point, and **WS2** in the middle of the slab [9], just next to accelerometers **A3** and **A2** from the dynamic monitoring system. Both sensors are supported by masts $3\,m$ high in order to reduce the interferences from the structure in the flow. As the wind observation is just made at one level, the wind sensors are mounted on top of the masts to avoid direct mast shadowing [15]. In this application,

a sampling rate of $10\,Hz$ was chosen in order to efficiently measure the turbulent component of the wind flow [15].

3.2 Permanent monitoring of the dynamic response

The dynamic monitoring system is set to acquire the data of the six accelerometers conveniently placed on the west slab to measure the vertical acceleration at six points at a sampling frequency of $20\,Hz$. Once it is configured, the acquisition system is capable of continuously measuring the vertical accelerations with no further user interaction. In the present application, the system is programmed to gather the measured data and save them in text files containing one hour length acceleration time series. These files are then hourly processed by an autonomous monitoring application specially developed to track the dynamic properties of the suspension roof [6, 8]. As result of the autonomous processing and identification of the raw data files, a set of dynamic properties is obtained as, for instance, the modal parameters and maximum and **R**oot **M**ean **S**quare (**RMS**) values of the measured accelerations. The permanent dynamic monitoring system consists of a data acquisition system installed on the west slab of the suspension roof and the autonomous monitoring application which was specially developed to automatically handle the great volume of data available in a permanent dynamic monitoring. The most notorious element of the permanent monitoring system is the autonomous monitoring application which was initially developed in Matlab® platform and, afterwards converted into a java® platform application [16] aiming at taking the best out of this platform as, for instance, its well-known robustness and flexibility on performing database and internet operations.

The whole transformation of the measured dynamic responses into relevant information regarding the evolution of the health of the monitored structure is depicted in Figure 5. The autonomous monitoring application is composed by several algorithms that are organized in three modules: (i) the data acquisition module, which is responsible for establishing a remote connection through the internet with the data acquisition system, transferring the available raw data files, checking their validity, storing them in a backup hard disk and pre-processing them in order to remove the trends, filter the signals according specified cutoff frequency, etc.; (ii) the automatic processing module, which is the core of the autonomous monitoring application as it is actually responsible for transforming the raw data acquired by the data acquisition system into relevant information regarding the health of the monitored structure; and (iii) the visualization module that consists of a **G**raphical **U**ser **I**nterface **GUI**-Toolbox called "*DynaMo Viewer*" that was developed in Matlab® platform to allow the visualization of the results automatically tracked by the processing module. The data acquisition and the processing modules are embedded in the latest release of the autonomous monitoring application illustrated in Figure 6. It consists of a computer program that was developed to run as tray application on the windows operating system and it was designed to consume as minimum processing resources of the hosting

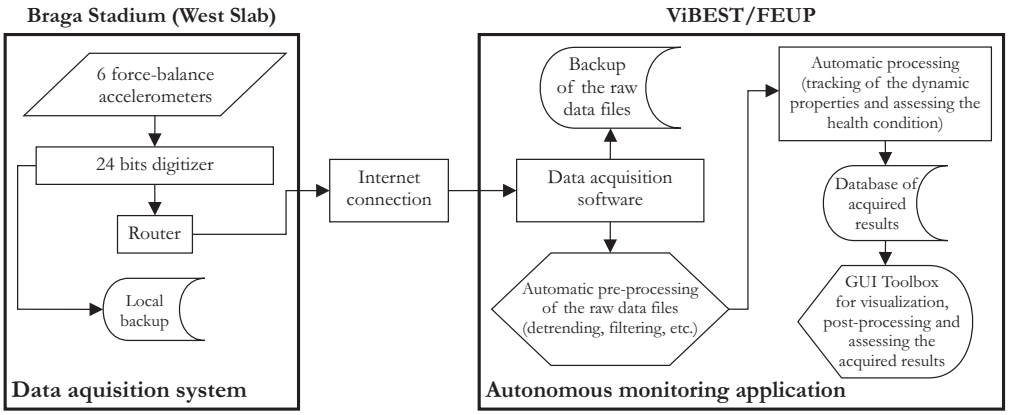

Figure 5: Data flow of the dynamic monitoring system installed on the west slab of the Braga stadium suspension roof.

computer as possible. One of the main advantages of a tray application like this is the fact that it runs in background, allowing the user of the host computer to perform other tasks while the application runs minimized in the tray. The application is set to automatically track the modal properties of the monitored structures using four state of art **M**odal **P**arameter **E**stimation (**MPE**) techniques as **SSI-COV**, **SSI-DATA** [17], **p-LSCF** [11, 1] and **EFDD** [18, 19]. In the case of the permanent monitoring of the Braga Stadium suspension roof the autonomous monitoring application is set automatically to establish a connection every hour with the router available in the data acquisition system, check whether there are new acquired raw data files, transfer and process the latest raw data files, and, finally, save the tracked results in the database of dynamic properties. Once these properties are saved in the database, they can be visualized by means of the GUI-Toolbox illustrated in Figure 7.

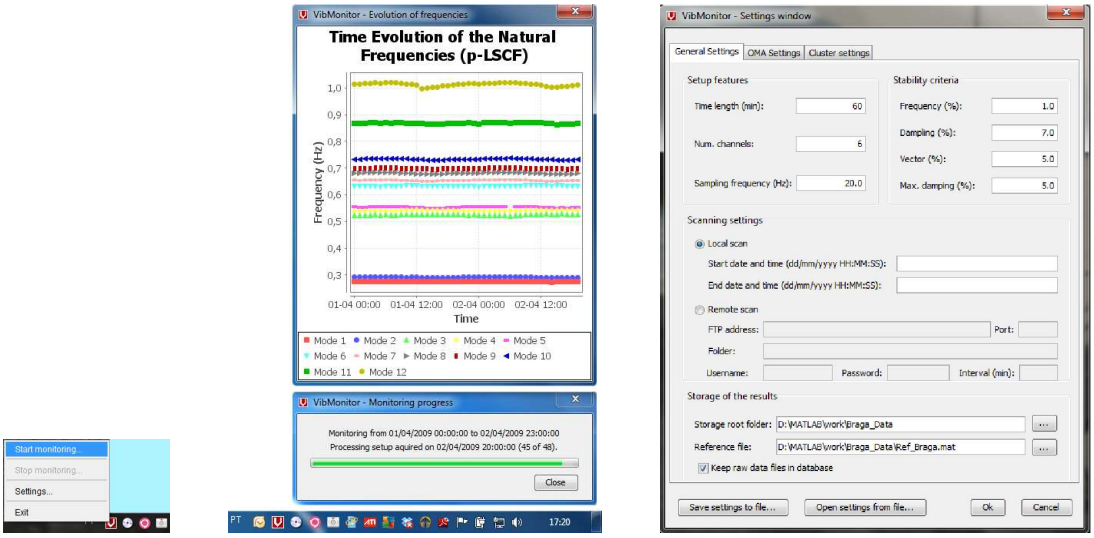

(a) (b) (c)

Figure 6: Autonomous monitoring application developed in java platform:(a) main popup menu of the tray application; (b) window showing the time evolution of the natural frequencies; and (c) settings window.

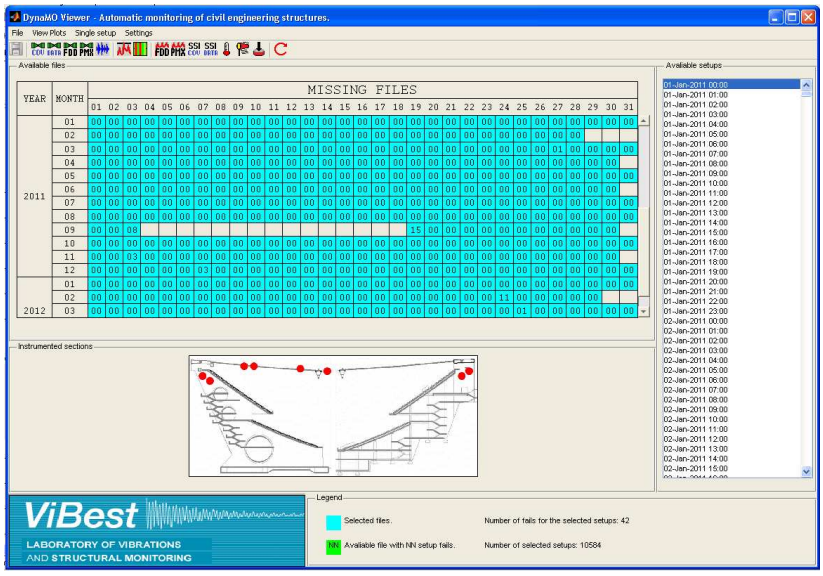

Figure 7: Overview of the database of setup files automatically processed by the autonomous application along of one year of monitoring.

The GUI-Toobox is composed of a total of 17 windows which are divided into a main, a configuration, a

release information and the other 14 windows that are used to display a specific property available in the database of results as, for instance, the time evolution of the natural frequencies and damping ratios, the time variation of RMS and Maximum values of measured accelerations, the correlations between the dynamic properties and environmental effects, etc. The main window, among other utilities, is used to open and activate the other windows, show an overview of the database and allow the selection of the setups available in the database [20].

3.3 Automatic tracking of the dynamic properties

Due to the large amount of data involved in the continuous monitoring of the roof structure, an autonomous monitoring application was used to automatically process and extract relevant information from the raw data files. The automatic identification of the modal parameters is one of the most important tasks executed by the autonomous application. Several techniques are found in the literature regarding the automatic extraction of the modal parameters by using the poles of the stability diagrams. In the case of the permanent monitoring of the Braga stadium suspension roof, some of these state-of-art techniques were tested to verify their efficiency, accuracy and robustness. These techniques are commonly based on hierarchical clustering algorithm [14] and the difference among them essentially relies on the criteria used to measure the degree of similarities of the mean properties of two clusters. Despite the good results obtained with the algorithm presented in [21], in the present application it was followed a similar approach, but adopting slightly different criteria, as defined by the following equations:

$$\begin{aligned} F(f_i, f_j) &= 2\frac{|f_i - f_j|}{f_i + f_j} \\ V(v_i, v_j) &= 1 - MAC(v_i, v_j), \end{aligned} \tag{1}$$

where $F(f_i, f_j)$ and $V(v_i, v_j)$ are, respectively, scalars that measure the degree of similarity between the mean frequencies and mean modal vectors of two clusters denoted by the indexes i and j, and f_i and f_j are the mean frequencies of these clusters. $MAC(v_i, v_j)$ is the modal assurance criterion and is used to calculate the correlation between two modal vectors by means of the following equation:

$$MAC(v_i, v_j) = \frac{|v_i^H v_j|^2}{(v_i^H v_i)(v_j^H v_j)}\,, \tag{2}$$

where v_i and v_j are, respectively, the mean modal vectors of the clusters i and j, and $(\bullet)^H$ denotes the transpose conjugate of a complex vector. The summation of eqs. 1 yields the following equation:

$$S_{ij} = F(f_i, f_j) + V(v_i, v_j)\,, \tag{3}$$

where S_{ij} is a value that measures the total degree of similarity between the mean properties of two clusters. The closer this value is to zero, the more similar the clusters of poles denoted by indexes i and j are. An interesting property of the equation used to calculate the differences in the natural frequencies is the fact of providing a quantification of the relative difference that does not depend on the order of comparison of the clusters of poles (e. g., order ij or ji). In the adopted implementation, this stability provided robust and accurate results on gathering the clusters of poles with similar modal properties. The result of a cluster analysis of the poles of typical stability diagram is shown in Figures 8a and 8b. It illustrates the automatic extraction of the modal properties of the suspension roof from the dataset acquired on 01/12/2011 at 00:00.

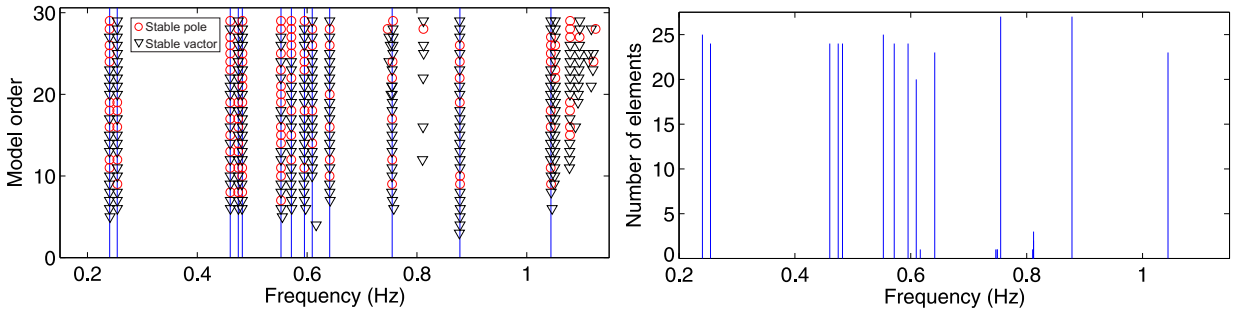

(a) (b)

Figure 8: Automatic tracking of the modal parameters using the poles of the stability diagrams constructed by means of p-LSCF technique using the setups acquired on 01/12/2011 at 00:00: (a) identification of the poles with similar modal properties and (b) the corresponding cluster analysis.

3.4 Results provided by the dynamic monitoring system

The autonomous monitoring application automatically tracked the modal properties of 8.400 raw data files along one year of monitoring from 01/01/2011 to 31/12/2011 with very few identification failures by means of four MPE techniques. One-year evolution of the natural frequencies in the range of $0-1\,Hz$ identified by means of p-LSCF method is illustrated in Figure 9. In Figure 10, a ten-day variation of the natural frequencies of modes 3, 4 and 5 due to the influence of environmental factors on the modal properties is clearly visible. This influence is also visible in the histograms containing the dispersions of the damping ratios automatically identified during one year of monitoring as illustrated in Figure 11. Another interesting aspect regarding the time evolution of the modal properties is that the pattern of variation of the natural frequencies observed for modes 3 and 4 are different from the other modes, as shown in Figure 10. This unexpected behaviour might be explained by the complex non-linear structural behaviour of the suspension roof. The statistics of one year of automatic tracking of the modal parameters are summarized in Table 1. It is worth noting that the highest standard deviations of the natural frequencies are observed for the modes 5, 6, 8, 9, 10, 11 and 12, which demonstrates that these modes seem to be more sensitive to the variation of the environmental conditions.

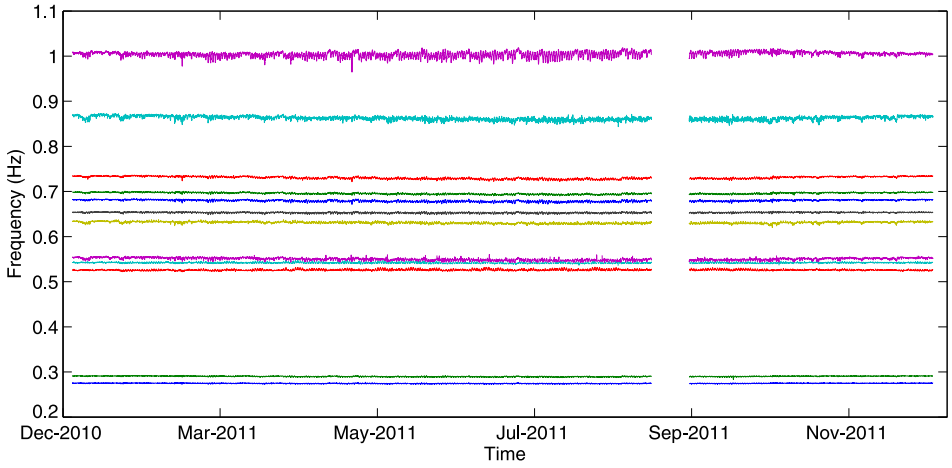

Figure 9: Time evolution of the natural frequencies automatically tracked for 12 modes in the range of $0-1\,Hz$ along one year of monitoring from 01/01/2011 to 31/12/2011.

d

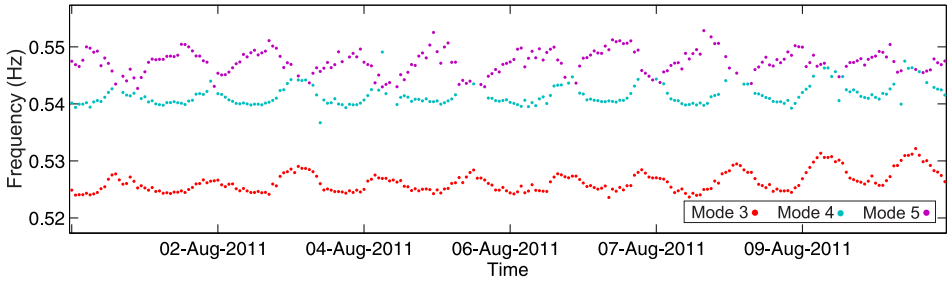

Figure 10: Time evolution of the natural frequencies automatically tracked for modes 3, 4 and 5, along 10 days of monitoring from 01 to 10/08/2011.

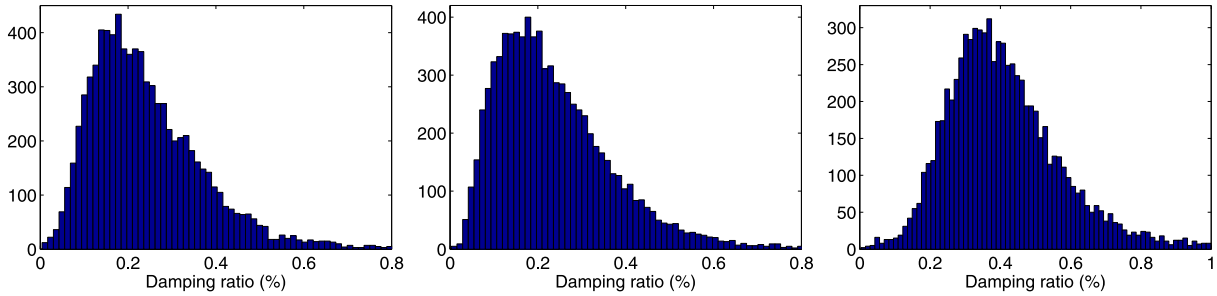

(a) (b) (c)

Figure 11: Dispersion of the modal damping values of modes: (a) 1, (b) 2 and (c) 5.

	Natural frequency		Damping ratio	
Mode	Mean (Hz)	Std. dev. (Hz)	Mean (%)	Std. dev. (%)
1	0.2746	0.0006	0.250	0.149
2	0.2906	0.0009	0.241	0.152
3	0.5261	0.0015	0.299	0.150
4	0.5420	0.0013	0.212	0.136
5	0.5503	0.0028	0.426	0.183
6	0.6310	0.0021	0.395	0.184
7	0.6531	0.0012	0.198	0.111
8	0.6795	0.0021	0.231	0.116
9	0.6958	0.0020	0.147	0.089
10	0.7306	0.0028	0.182	0.106
11	0.8623	0.0044	0.431	0.194
12	1.0045	0.0055	0.459	0.147

Table 1: Mean values and standard deviations of the natural frequencies and damping ratios experimentally identified from 01/01/2011 to 31/12/2011 (p-LSCF).

3.5 Analysis of wind characteristics

The field measurements from the two three-dimensional ultrasonic anemometers are continuously recorded by the wind observation system. These sensors measure the three orthogonal components of the wind instantaneous velocity in the sonic anemometer referential and the sonic temperature.

3.5.1 Mean wind speed, direction and incidence

In order to obtain the mean wind speed, direction and incidence angles in a conventional time interval (10 or 60 minutes along this study), as well as the turbulent time series for the longitudinal, lateral and vertical direction for the same period, a coordinate rotation algorithm is applied. For this study, it was used a double coordinate rotation scheme [15, 22]. The time-history of mean wind speed measured by both anemometers, during the period of five months, from the 8^{th} of December 2011 to the same day of May 2012, is shown in Figure 12. From this graphic, it's possible to conclude that the mean wind velocities measured are relatively low, with maximum values of $9.37\,m/s$ and $7.22\,m/s$ for wind sensors **WS1** and **WS2**, respectively. Looking at Figure 12b, where just the mean wind speeds greater than $4\,m/s$ are represented, it is clear the prevalence of measured data from wind sensor **WS1** on the highest values.

Figure 13 shows the distribution of the mean wind direction with mean wind speed for average times of 10 minutes. It is clear from Figure 13a that the vast majority of measured data points are condensed in the low velocity range. By removing the data points with mean wind speeds inferior to $4\,m/s$ (Figures 13b and 14a) clear trends are observed. Once again, it is visible the dominance of data points from sensor **WS1** on the higher range of wind speeds. For this sensor, the strongest winds were measured coming from the north-northwest direction, with some lower speeds from south and east. The sensor **WS2** registered the stronger winds coming from the north and south directions.

Figures 14b and 14c show the distribution of the wind incidence angle for the mean wind speed and mean wind direction respectively. Wind sensor **WS1** registered incidence angles between -5 and 10 degrees (where positive values represent ascending winds). For wind sensor **WS2** the range is much wider, particularly for the positive values, with a good deal of data points between 10 and 25 degrees. For both cases the incidence angles can be separated in two almost distinct clusters, one mostly with negative values and another exclusively with positive values. This distribution is better understood by analysing Figure 14c. The negative incidence angles are almost exclusive for winds from south-east, while positive angles are connected with winds coming from north-northwest.

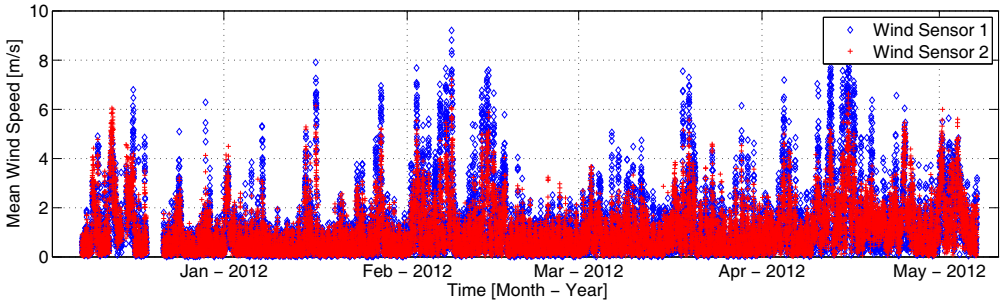

(a)

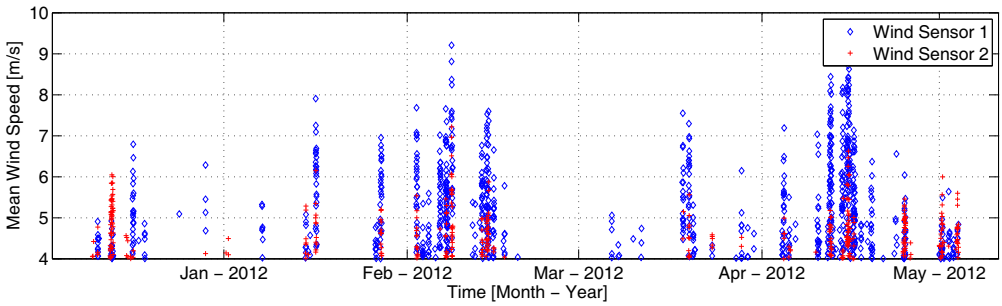

(b)

Figure 12: Time-history of 10-min mean wind speed measured by the 2 sonic anemometers over the period of 5 months: (a) Complete range of mean wind speeds; (b) 10-min mean wind speed greater than $4\,m/s$.

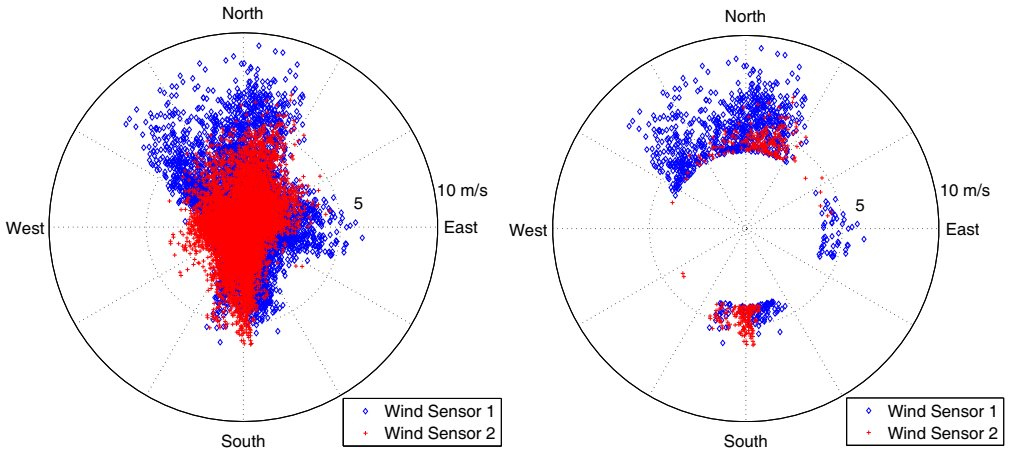

Figure 13: Wind rose diagrams of 10-min mean wind direction and speed for the two sonic anemometers: (a) Complete range of mean wind speeds; (b) 10-min mean wind speed greater than $4\,m/s$.

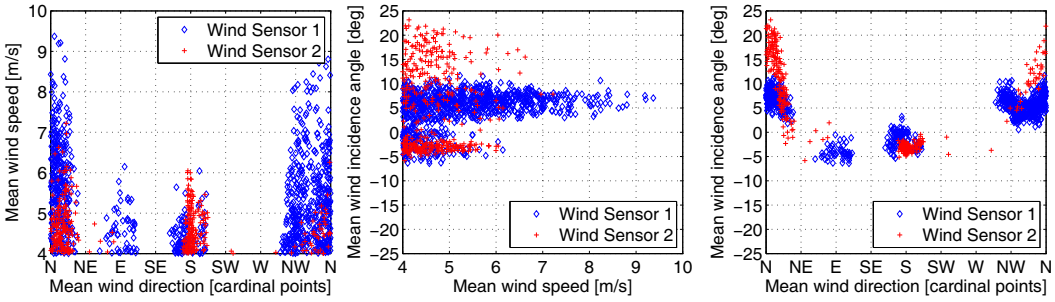

Figure 14: (a) Distribution of 10-min mean wind speed with direction; Distribution of 10-min mean wind incidence angle with: (b) mean wind speed; (c) mean wind direction.

These results are in accordance with the expected for the structure's implantation in the terrain and the sensors position on the structure. As the stadium is positioned along the northeast-southwest axis (see Figure 4), and the anemometers located on the west slab, the south winds come from the top of the west slab, and so they must have descending incidence, while the winds coming from north-northwest come from the stadium open side and reach the anemometers with ascending incidence. The high incidence angles measured by the wind sensor **WS2** (located on the middle of the west slab) show the influence of the structure on the north-northwest winds flow.

3.5.2 Turbulence intensity

The longitudinal, lateral and vertical turbulence intensities can be determined by the following equations:

$$I_u = \frac{\sigma_u}{U}, \quad I_v = \frac{\sigma_v}{U}, \quad I_w = \frac{\sigma_w}{U} \tag{4}$$

where σ_u, σ_v and σ_w are the standard deviation or the RMS of each fluctuating velocity component and U the wind mean speed for the same time period.

Figure 15 shows the variation of the turbulence intensity in the longitudinal, lateral and vertical directions with the 10-min mean wind speed, for both sonic anemometers. Values computed for wind sensor **WS2** present a bigger spread and higher turbulence intensities for the lower wind speeds. Turbulence intensities from wind sensor **WS1** show a clear tendency to decrease for higher mean wind speeds in every direction.

The same tendency is present in data from wind sensor **WS2**, although with less expression due to the lower mean wind speeds observed. The ratios between the averaged values of the turbulence intensity in the three directions are $\sigma_u : \sigma_v : \sigma_w = 1 : 0.847 : 0.530$ for wind sensor **WS1** and $1 : 0.830 : 0.523$ for wind sensor **WS2**, which are close to the ratios proposed by Solari [23].

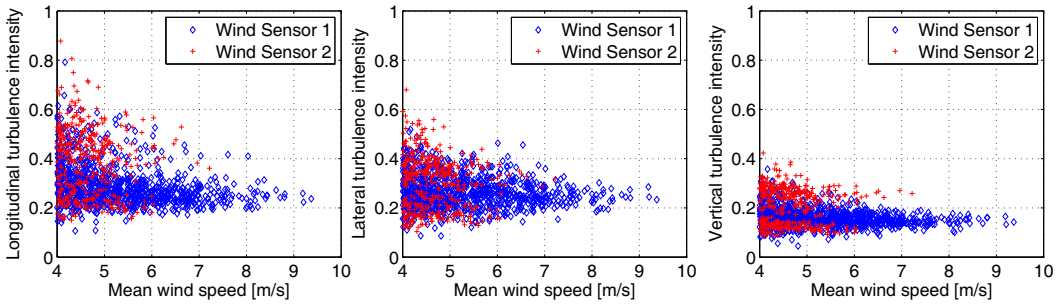

(a) (b) (c)

Figure 15: Relationship between the turbulence intensity and 10-min mean wind speed measured by the two sonic anemometers: (a) Longitudinal turbulence intensity; (b) Lateral turbulence intensity; (c) Vertical turbulence intensity.

4 Correlations between the dynamic response and the wind characteristics

4.1 Wind velocity *vs* west slab vertical acceleration

Figure 16 shows the relationship between the 10-min mean wind speed registered by wind sensor **WS1** and the RMS of the vertical accelerations measured in three different locations, namely the three accelerometers positioned along the west slab inner edge (accelerometers **A1**, **A2** and **A3**, in Figure 4). From the three figures one can observe a general trend in the vertical acceleration to increase for higher wind velocities. This trend is best fitted, in every case, by a quadratic function. It is noticeable that the accelerometers **A1** and **A3** show greater values of RMS accelerations for the same mean wind speed than accelerometer **A2**. This is due to the modal shape configuration of the dynamic modes more excited by the wind.

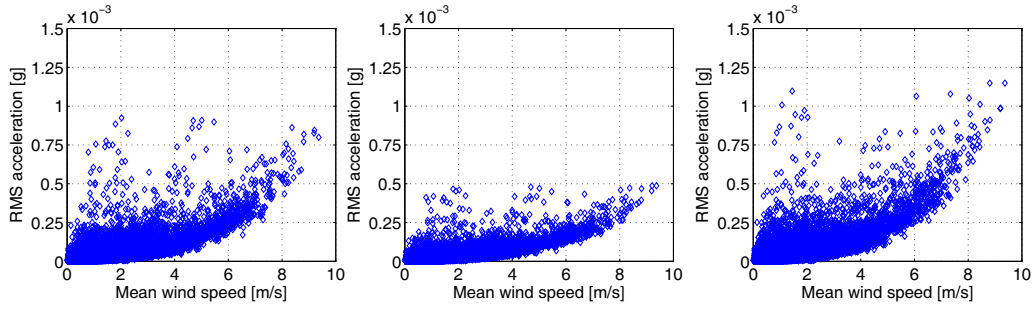

(a) (b) (c)

Figure 16: Relationship between the 10-min mean wind speeds measured by wind sensor WS1 and the RMS vertical acceleration responses for: (a) accelerometer A1; (b) accelerometer A2; (c) accelerometer A3.

4.2 Wind velocity *vs* identified damping ratios

Figure 17 presents the relationship between the 60-min mean wind speed registered by wind sensor **WS1** and identified modal damping ratios for the same period of time. In this figure the damping ratios for the

2^{nd}, 9^{th} and 12^{th} mode are represented. A clear increasing trend regarding the variation of the damping ratio with the mean wind speed can be observed on most of the identified vibration modes, as represented in Figure 17 for the 2^{nd} and 12^{th} modes. Meanwhile, for a minority of the identified vibration modes, like the 9^{th} (Figure 17b), the damping ratio has small or no increase.

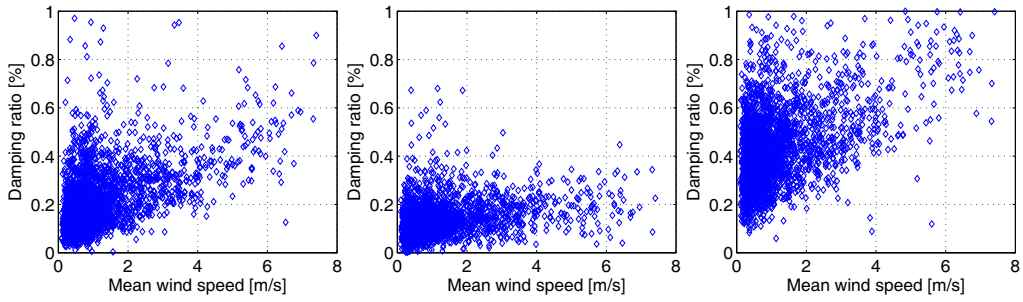

Figure 17: Relationship between the 60-min mean wind speeds measured by wind sensor WS1 and the damping ratios computed for the same period of time for: (a) 2^{nd} mode; (b) 9^{th} mode; (c) 12^{th} mode.

4.3 Wind incidence *vs* identified frequencies

In some of the identified vibration modes, the representation of the distribution of the mode natural frequency with the mean wind incidence angle is similar to the one regarding the 2^{nd} mode and from wind sensor **WS1**, shown in Figure 18b. In Figures 18a and 18b one can identify two distinct data point groups: one above the 0 degrees incidence angle, with identified frequencies between $0.287\,Hz$ and $0.290\,Hz$, and a second group with negative incidence angle and natural frequencies between $0.289\,Hz$ and $0.291\,Hz$. However, the tendency for higher frequencies with the negative incidences cannot be verified, as Figures 18a and 18c show a decreasing trend of the natural frequency with the mean wind speed.

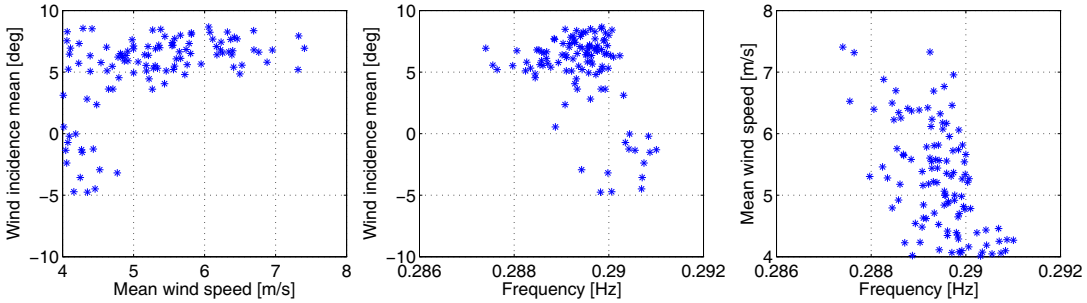

Figure 18: Relationship between the 60-min mean wind speed, incidence measured by wind sensor WS1 and the computed frequency for the 2^{nd} mode.

5 Conclusions

The autonomous monitoring software was able to automatically track the modal parameters in the frequency range of $0-1\,Hz$ along one year of monitoring by means of 4 different techniques with very few identification failures. The characterization of the variation of modal properties along the time has demonstrated the reliability, robustness and precision of the developed application to track the modal properties of the suspension roof. The assessment of the time evolution of the modal properties of the suspension roof showed that the natural frequencies of modes 3 and 4 vary proportionally with the daily and seasonal variations of the environmental temperatures. This unexpected behaviour might be explained by the complex non-linear

structural behaviour of the suspension roof. With regard to the implemented wind measurement system, it has been working for less than six months and is part of ongoing project, so the results presented in this paper should be considered as preliminary. Nevertheless, some important conclusions can be drawn from the measured data. During the measurement time frame, the mean wind speeds recorded were relatively low. Wind sensor **WS1** (located on the slab corner) registered the highest mean wind speeds, with a predominance of the north-northwest direction, while wind sensor **WS2** measured much smaller mean wind speeds with north and south directions. The wind flow measured by wind sensor WS2 has demonstrated to be more influenced by the stadium structure, fact that can be observed in the very wide spread from the positive wind incidence angle and by the higher turbulence intensities in the lower wind speeds. The RMS of the vertical accelerations of the slab showed a clear increasing trend for higher mean wind speeds measured by wind sensor **WS1**, which can be fitted by a quadratic function. The analysis of the correlation between identified modal damping rations and the mean wind speed captured by **WS1** has evidenced an increasing trend with the mean wind speed for several, although not all of the modes. The continuous long-term wind measurement will allow the validation of the wind model developed at the design stage and to establish better correlations with the identified modal parameters. Although partial, the cross analyses between the data acquired by both systems have evidenced a significant influence of the wind action on dynamic properties of the roof structure.

Acknowledgements

The authors would like to acknowledge: (1) all the support provided by the Portuguese Foundation for Science and Technology (FCT) to ViBest / FEUP for the development of research in the area of Long-Term Dynamic Monitoring, and particularly within the Scientific Re-equipment Project “Dynamic Behaviour Monitoring for Structural Safety Assessment / National Network of Geophysics”, as well as (2) for the development of the Research Projects “Wind analysis of special structures from full scale measurements” (PTDC/ECM/102087/2008) and “DYNAMO_DEMO - Advanced Tools for Dynamic Structural Health Monitoring of Bridges and Special Structures” (PTDC/ECM/109862/2009); (3) the Ph.D. Scholarship (SFRH/BD /44291/2008) provided by FCT to the first author; and (4) all the cooperation from the design office AFA Consult, as well as from the local authorities of “Câmara Municipal de Braga”.

References

[1] F. Magalhães, *Operational modal analysis for testing and monitoring of bridges and special structures* (Ph. D. thesis), Faculty of Engineering of the University of Porto, Porto, Portugal (2010).

[2] W. Hu, *Operational modal analysis and continuous dynamic monitoring of footbridges* (Ph. D. thesis), Faculty of Engineering of the University of Porto, Porto, Portugal (2011).

[3] E. Reynders, J. Houbrechts and G. De Roeck, *Fully automated (operational) modal analysis*, Mechanical Systems and Signal Processing, Vol. 1, No. 29 (2012), pp. 228-250.

[4] E. Caetano, A. Cunha and F. Magalhães, *Numerical and experimental studies of Braga sports stadium suspended roof.* Journal of Structure and Infrastructure Engineering, Vol. 6, No. 6 (2010), pp. 715-724.

[5] F. Magalhães, E. Caetano and A. Cunha, *Operational modal analysis and finite element model correlation of the Braga Sport Stadium Suspended roof,* Engineering Structures, Vol. 1, No. 30 (2007), pp. 1688-1698.

[6] F. Magalhães, A. Cunha and E. Caetano, *Installation of a Continuous Dynamic Monitoring system at Braga Stadium Suspended Roof: initial results from automated modal analysis*, IOMAC 2009, Ancona, Italy (2009).

[7] E. Caetano and A. Cunha, *Numerical modeling of the structural behaviour of the new Braga Stadium roof* (Technical Report), FEUP/VIBEST, Porto, Portugal (2001).

[8] S. Amador, F. Magalhães, E. Caetano and A. Cunha, *Analysis of the influence of environmental factors on modal properties of the Braga Stadium suspension roof*, EVACES 2011 - Experimental Vibration Analysis for Civil Engineering Structures, Varenna, Italy (2011).

[9] N. Martins, A. Cardoso and E. Caetano, *Development of an observation system based on anemometry to characterize the wind action over a suspension roof*, YIC2012 - First ECCOMAS Young Investigators Conference, Aveiro, Portugal (2012).

[10] S. Amador, *Operational Modal Analysis Studio 2010 - User's Guide, ViBEST/FEUP*, Porto, Portugal (2010).

[11] B. Peeters, H. Van Der Auweraera, F. Vanhollebeck and P. Guillaumec, *Operational modal analysis for estimating the dynamic properties of a stadium structure during a football game*, Shock and Vibration, Vol. 1, No. 14 (2007), pp. 283-303.

[12] E. Reynders, F. and Magalhães, G. Roeck and A. Cunha, *Merging Strategies for multi-setup operational modal analysis: application to the Luiz I steel arch bridge*, Proceedings of the 27th International Modal Analysis Conference (IMACXXVII), Society for Experimental Mechanics, Orlando, Florida, US (2009).

[13] M. Döhler, E. Reynders, F. Magalhães, L. Mevel, G. De Roeck and A. Cunha, *Pre- and Post-identification Merging for Multi-Setup OMA with Covariance-Driven SSI*, Proceedings of the 28th International Modal Analysis Conference (IMACXXVIII), Society for Experimental Mechanics, Jacksonville, Florida, USA (2010).

[14] C. F. Olson, *Parallel algorithm for hierarchical Clustering. Parallel Computing*, Vol. 1, No. 21 (1995), pp. 1313-1325.

[15] J. C. Kaimal and J. J. Finnigan, *Atmospheric boundary layer flows: their structure and measurement*, New York, Oxford University Press, USA (1994).

[16] Oracle, *The Java EE 6 tutorial* (2012).

[17] B. Peeters, *System Identification and Damage Detection in Civil Engineering* (Ph. D. thesis), Katholieke Universiteit Leuven, Leuven, Belgium (2000).

[18] R. Brincker, C. E. Ventura and P. Andersen, *Damping Estimation by Frequency Domain Decomposition*, Proceedings of The 19th International Modal Analysis Conference (IMACXIX), Society for Experimental Mechanics, Orlando, Florida, USA (2001).

[19] R. Brincker, P. Andersen and N. J. Jacobsen, *Automated Frequency Domain Decomposition for Operational Modal Analysis*, Proceedings of The 25th International Modal Analysis Conference (IMACXXV), Society for Experimental Mechanics, Orlando, Florida, USA (2007).

[20] S. Amador, *Dynamo Viewer Uses's Guide: A Graphical User Interface for Long Term Dynamic Monitoring of Civil Engineering Structures*, ViBEST/FEUP, Porto, Portugal (2009).

[21] F. Magalhães, E. Caetano and A. Cunha, *Online automatic identification of the modal parameters of a long span arch bridge*, Mechanical Systems and Signal Processing, Vol. 23, No. 2 (2009), pp. 316-329.

[22] J. M. Wilczak, S. P. Oncley and S. A. Stage, *Sonic anemometer tilt correction algorithms*, Boundary-Layer Meteorology, Vol. 99, No. 1 (2001), pp. 127-150.

[23] G. Solari and G. Piccardo, *Probabilistic 3-D turbulence modeling for gust buffeting of structures*, Probabilistic Engineering Mechanics, Vol. 16, No. 1 (2001), pp. 73-86.